TRACKING PROBLEM FOR EYE MOVEMENT

by

SAMANMALEE SUGATHADASA, B.E.

A THESIS

IN

MATHEMATICS

Submitted to the Graduate Faculty
of Texas Tech University in
Partial Fulfillment of
the Requirements for
the Degree of

MASTER OF SCIENCE

Approved

Accepted

August, 1999

ACKNOWLEDGEMENTS

I would like to thank Professor Clyde F. Martin for his guidance and encouragement in this research, both as a thesis advisor and as a teacher. His enthusiasism and avid interest in the subject promoted a very exciting atmosphere. Also I wish to thank Dr. Lawrence Schovenec for his advice and for serving as a member of my thesis committee. I owe special thanks to the Department of Mathematics at the KTH, Stockholm, and particularly to the chair, Professor Anders Lindquist, for the opportunity provided to pursue this work during the first half of the summer of 1999. Last, but not least, I would like to thank my husband Dr. W. P. Dayawansa for his encouragement.

My thesis is dedicated to Daya, Samantha, Tamara and Nuwan.

CONTENTS

ABSTRACT

The eyes move in order to place an intended object on the region of the retina with greatest visual acuity, called the fovea. Movement of eyes are produced via the coordinated action of several muscle groups acting in response to neurological signals. The focus of this thesis is to study a particualr type of eye movement called smooth pursuit from the perspective of control theory.

There are several types of eye movements reported in the research literature. Primarily among them are the (1) saccadic or fast eye movement subsystem (2) pursuit or tracking subsystem (3) vergence subsystem (4) vestibular subsystem. In contrast to the saccadic eye movement research, scant attention has been paid to the study of the remaining types from the viewpoint of control. Here a detailed description is given on how to design a controller for the pursuit eye movement using an occular motor plant model from recent research literature. This model represent capabilities of muscle actuators of the eyes reasonably accurately from the viewpoint of their actuator and length limitations and other nonlinearities, but disregards details of cortical circuitry behind signal generation. Performance of the designed controller is demonstrated via simulations pertinent to pursuit of sinusoidal. ramp and parabolic signals. It is argued that the designed controller performs better than the actual occular motor plant for the reason that the aditional restrictions imposed by cortical circuitry are completely disregarded in the design. Overall, the latency and peak velocity of the designed controller is shown to be within a factor of four of the actual occular motor controller during pursuit.

LIST OF FIGURES

CHAPTER I
INTRODUCTION

The eyes move in order to place an intended object on the region of the retina with greatest visual acuity, called fovea. Movement of eyes are produced via the coordinated action of several muscle groups acting in response to neurological signals. The focus of this thesis is to study a particular type of eye movement called smooth pursuit from the perspective of control theory.

When looking back over the past 15 years it is clear that eye movement research has been quite influential across several domains. Research on the reading process has benefited significantly from insights obtained from eye movement data (see e.g. , [19]) as well as research on scene perception, visual search, and other perceptual and cognitive processes. Today, the need to understand the ocular motor control system stems from two important research areas: biomedical engineering and the design of systems capable of taking eye-gaze commands. Biomedical engineering is inching toward the point of artificially stimulating muscle groups in order to correct defects, whereas designers of sophisticated equipment under visual commands are fast reaching the point where the dynamics of eye movement is a primary factor in speeding up the response times.

There are several types of eye movements reported in the research literature. For example Troost [23] (see also [25, 26, 24, 21, 5] for additional detail) describe four subsystems of the supranuclear ocular motor control (i.e., distinction originates in the higher regions of the brain): (1) saccadic or fast eye movement subsystem, (2) pursuit or tracking subsystem, (3) vergence subsystem, (4) vestibular subsystem. **Saccades** are rapid binocular eye movements which are under both voluntary and reflex control. The visual stimulus for a saccade is the displacement of the target object. Typically saccades occur with a latency of 200 to 250 msec after an instantaneous displacement of the target. Saccades are ballistic (i.e., under open-loop control, and cannot be

redirected once the motion is initiated) and the peak velocity can range from 30^0/sec to 700^0/sec with up to 40^0 amplitude. Eye movement during a saccade is relatively simple: an appropriate latency followed by a period of acceleration to peak velocity followed by decceleration of the eyes onto the new target position. Correspondingly, the control action taken is also relatively simple. The second type, the **pursuit** eye movement, is evoked by the slow movement of a fixated target after a latency of about 125 msec. Maximum eye velocity can go up to 50^0/sec. In contrast to saccadic eye movement pursuit eye movement is smooth, and can be continuously modified in response to visual input (i.e., under feedback control). Retinal velocity error is thought to be the input signal to the pursuit control system. This suggestion is corroborated with physiological evidence that demonstrate that pursuit cannot be initiated voluntarily, i.e., without an actual target motion. Attempts to initiate pursuit voluntarily leads to a series of small saccades called the "cog-wheel" pursuit. The third type, the **vestibular-occular** eye movement, occur as a compensatory response to a head movement, and is elicited by the vestibular system. The latency can be up to 100 msec and the peak eye velocity can be as fast as 300^0/sec. In general, the eyes move in an opposite direction to the movement of the head, and the counterrotation, which may match exactly under well lit conditions, takes place as a smooth movement under continuous feedback control interrupted by intermittent saccades that recenter the eyes toward midposition in the orbit. It is thought that the head acceleration is the input signal during the feedback control (i.e., continuous) phase. The fourth type, the **Vergence** eye movement, occur in response to motion toward or away from the observer. The latency is approximately 160 msec and the maximum velocity is about 20^0/sec.

There is much biological evidence to suggest that the smooth pursuit eye movement and the saccadic eye movement are fundamentally different neurological phenomena, among them are are the region of origin of control signals in the brain (see e.g. [22]) and the pathways (for example, it is reported in [23] that horizontal saccades originate in the cortex of the contralateral frontal lobe, whereas pursuit originate in

the ipsilateral parieto-occipital visual association areas). Differences have been found regarding the other types eye movements as well (see e.g., [23]).

Among the four types of eye movements described above there have been extensive investigations aimed at understanding the saccadic eye movement from a variety of viewpoints (see e.g., [15] and references therein, or the 60 odd papers listed and references therein in [12]). There have been many recent investigations aimed at understanding the saccadic movement of the eye from the viewpoint of control theory (see e.g., [17, 16, 18, 9], etc.). Modeling the eye as a control system involves taking into account the nature of the neural signals, dynamics of the eye balls and the surrounding medium, and nonlinear dynamics of the muscles and their inherent limitations on length and generation of force, resulting in a fairly complicated mathematical model. In spite of this, as had been indicated above, saccadic eye movement is fairly simple to analyze from the viewpoint of control theory. Primarily one only need to find amplitudes and durations of constant control signals during acceleration, coasting and deceleration periods. In contrast analysis of other types of eye movements are far more complex. Since some type of feedback control is involved in all these types one can safely assume that understanding pursuit control system is a prerequisite to understanding vestibulo-ocular and vergence eye movements as well. In this thesis the task of proposing a mathematical model in order to generate neural control signals to produce pursuit eye movement is undertaken. As far as we are aware this is the first such attempt which takes into consideration anatomically accurate models of relevant muscle groups.

Modeling of the human ocular system and its dynamic properties has been addressed by many scientists. In 1630, Descartes[10] developed one of the first models of eye movement based on the priciple of reciprocal innervation, a notion of paired muscular activity in which a contraction of one muscle is associated with the relaxation of another. Descartes' basic idea has been expanded and modified to include varying levels of detail and sophistication. In 1954, Westheimer (see e.g., [7]) de-

veloped a linear second-order approximation of eye dynamics during a saccade. His model worked well for up to 10 degree saccades but not for larger saccades. Robinson [2, 1, 3] advanced a more realistic representation of eye movement consisting of a linear fourth-order model that could simulate saccades between 5 and 50 degrees, but the velocity profiles produced by this model were not physically realistic. Both Westneimer and Robinson acknowledged the eye movement mechanism to be inherently nonlinear due to the geometry of the system and the nonlinear physiological behavior of certain components pertaining to extraocular muscle. Another group of researchers proposed the Cook-Clark-Stark [8, 6] model which addressed the nonlinear relationships between force and velocity in the muscle and produced realistic position, velocity, and acceleration profiles. However, their model failed to incorporate certain force-length muscle characteristics which have recently gained prominence in the literature of bio-mechanical modeling. Later this model was modified by the addition of force-length relationship of muscle.

Perhaps the most realistic models of musculotendon actuators was proposed by Hill [14]. This model captures the nonlinear force-length relationship reasonably well, and has been used extensively in [27, 13] in modeling leg movement during jumping, and in modeling the saccadic eye movement in [9, 16, 18, 17]. Here a Hill-type model is used to represent muscle dynamics, and address the problem of finding control laws that make the pupil movement follow a given trajectory is addressed.

This thesis is organized as follows. In Chapter II, a mathematical model describing the occular motor control system is discussed. This model is taken from the M.S. thesis of A. McSpadden [17], and relevant features captured in the model include length and actuation force limitations and other nonlinearities of muscles, mass, stiffness and damping in the eye, and amplitude and rate limitations of neural input signals. This model disregards details of the origin and the cortical pathways of the neural signal. In Chapter III, a mathematical analysis of the pursuit eye movement is discussed with the aim of describing representative neural inputs generated in the

form of a feedback control law that would facilitate tracking a slowly moving target. To our knowledge this is the first such attempt, where the fundamental nature and limitations of muscles are represented accurately. No suggestion is made that these signals are comparable to actual neural signals. It is left to the experimentalists to verify this aspect. However, the fundamental ideas behind the design can be modified if one were to start from experimental data and recover the neural control signals from them. In Chapter IV, some simulation results from Matlab are presented to illustrate the performance of the controller designed in Chapter III. Tracking signals considered are two sinusoidal signals and a ramp signal. It is concluded that the performance of the controller is comparable to what has been reported in the research literature on pursuit eye movement. The Matlab programs used are reproduced in an Appendix.

CHAPTER II
THE OCCULAR MOTOR PLANT MODEL

There have been many recent studies aimed at modeling the dynamics of the eye movement (see e.g., [17],[11],[20],[9]). A common theme in all this work is to model the eye as a rigid body controlled by muscles attached to it. They differ in the way the muscles are modeled. It is our viewpoint that the nonlinear dynamics of muscles play a central role. In this regard, recent models developed by [17] are the most relevant.

In his M.S. thesis [17], A. McSpadden derived a system of dynamical equations to describe the eye movement in a horizontal plane. Attention is restricted to the medial rectus and lateral rectus muscles as actuators, and they were modeled using Hill's equations [14, 27]. The eye is modeled as a solid sphere with rotational innertia J_G, rotational viscocity B_G and linear spring constant K_G around a vertial axis through its center. It is assumed that the medial rectus and lateral rectus muscles have identical characteristics, each having a mass M. A schematic model is presented in Figure 2.1.

In [17], dynamical equations were derived to represent the model depicted in Figure 2.1, consisting of twelve coupled nonlinear differential equations with two neural control inputs. It was shown that a reasonably good approximation consisting of eight state variables can be derived in the form,

$$\dot{x} = f(x) + g_1(x)n_1(t) + g_2(x)n_2(t) \tag{2.1}$$

where, x represent the state vector, f, g_1 and g_2 are nonlinear vector fields to be described later, and n_1 and n_2 represent the neural input signals to the medial rectus and lateral rectus muscles, respectively.

The state vector of the occulomotor plant is $x = [\theta, \dot{\theta}, F_{t1}, F_{t2}, l_{m1}, l_{m2}, a_1, a_2]'$

where,

$$\begin{aligned}
\theta &= \text{eyeangle} \\
\dot{\theta} &= \text{angular velocity of the eye} \\
F_{t1} &= \text{tendon force of the medial rectus muscle} \\
F_{t2} &= \text{tendon force of the lateral rectus muscle} \\
l_{m1} &= \text{length of the medial rectus muscle} \\
l_{m2} &= \text{length of the lateral rectus muscle} \\
a_1 &= \text{activation level of the medial rectus muscle} \\
a_2 &= \text{activation level of the lateral rectus muscle.}
\end{aligned}$$

Of course, the state space is a proper subset of $\Re^8$ since several of the state variables have to satisfy hard constraints. For the sake of simplicity, only the following constraints are imposed here.

- Tendon forces are not allowed to fall below a minimum threshold level or exceed a maximum threshold level.
- Muscle lengths have to be between a lower and an upper limit.
- Neural activation levels of the medial rectus and lateral rectus muscles have to be between 0 and 1.

Dynamics of the occulomotor plant given in (2.1) are quite complicated. Below

we describe the vector fields f, g_1, and g_2:

$$f(x) = \begin{bmatrix} x_2 \\ (x_3 - x_4 - B_g x_2 - K_g x_1)/J_g \\ K_t(x_3)[-x_2 - (180/\pi)o(x_3, x_5, x_7)] \\ K_t(x_4)[x_2 - (180/\pi)o(x_4, x_6, x_8)] \\ \phi(x_3, x_5, x_7) \\ o(x_4, x_6, x_8) \\ -x_7/\tau \\ -x_8/\tau \end{bmatrix}. \tag{2.2}$$

$$g_1(x) = \frac{1}{\tau}[0, \cdots, 0, 1, 0]'.$$

$$g_2(x) = \frac{1}{\tau}[0, \cdots, 0, 1]'.$$

Here, τ represent a time constant reflecting the delay in converting neural signals to muscle activation signals, and K_t and o are nonlinear functions.

$$K_t(x) = \begin{cases} k_{te}x + k_{tl}: & 0 \le x \le F_{tc} \\ k_s: & x \ge F_{tc}, \end{cases} \tag{2.3}$$

$$\phi(x, y, z, w) = \begin{cases} V_{max}[\frac{x - F_{pe}(y)}{zF_{max}F_l(y)} - 1]^3: & z \ge c \\ \frac{-K_t(x)z}{v(y) + (180/\pi r)K_t(x)}; & z < c. \end{cases} \tag{2.4}$$

The function parameters F_{pe}, F_l and ψ in the expressions of o are given by.

$$\psi(l) = \begin{cases} \frac{k_{ml}}{k_{me}}[exp(k_{me}(180/\pi r)(l - l_{ms}): & l_{ms} \le l \le l_{mc}. \\ (180/\pi r)k_{pm}; & l \ge l_{mc}. \\ 0; & \text{otherwise.} \end{cases} \tag{2.5}$$

$$F_{pe}(l) = \begin{cases} \frac{k_{ml}}{k_{me}}[exp(k_{me}(180/\pi r)(l - l_{ms}): & l_{ms} \le l \le l_{mc}. \\ k_{pm}(180/\pi r)(l - l_{mc}) + F_{mc}: & l \ge l_{mc}. \\ 0; & \text{otherwise.} \end{cases} \tag{2.6}$$

$$F_l(l) = 1 - (\frac{l/l_{opt} - 1}{w})^2. \tag{2.7}$$

Approximate values of the constants appearing in the functions above were estimated in [17] to be:

Table II.1: Parameters and estimated values

parameter	description	value
r	radius of the eye	$1.24cm$
J_g	rotational innertia of the eye	$6 \times 10^{-5} gts^2/^0$
B_g	rotational viscocity of the eye	$0.0158 gts/^0$
K_g	rotational viscocity of the eye	$0.79 gt/^0$
B_{pm}	passive muscle viscosity	$0.06 gts/^0$
M	muscle mass	$0.748g$
F_{max}	maximum isometric muscle force	$100gt$
l_{mp}	primary muscle length	$4.0cm$
l_{opt}	optimal muscle length	$4.65cm$
l_{ms}	muscle slack length	$3.7cm$
l_{mc}	linear limit of passive muscle	$4.8cm$
k_{me}	a shape parameter	$0.0387/^0$
k_{pm}	linear passive muscle elasticity	$0.9 gt/^0$
k_{ml}	minimum passive muscle elasticity	$0.126 gt/0$
F_{mc}	linear limit of muscle force	$20gt$
w	a normalizing parameter	0.5
V_{max}	maximum muscle velocity	$5689^0/s$
k_s	linear tendon elasticity	$2.5 gt/^0$
k_{tl}	minimum tendon elasticity	$1.5 gt/^0$
k_{te}	a shape parameter for tendon force	$0.0333/^0$
l_{ts}	tendon slack length	$0.2cm$
l_{tc}	a shape parameter	$0.532cm$
F_{tc}	a shape parameter	$30gt$

These parameter values will be used in carrying out simulations reported in section 3.3 in the next chapter.

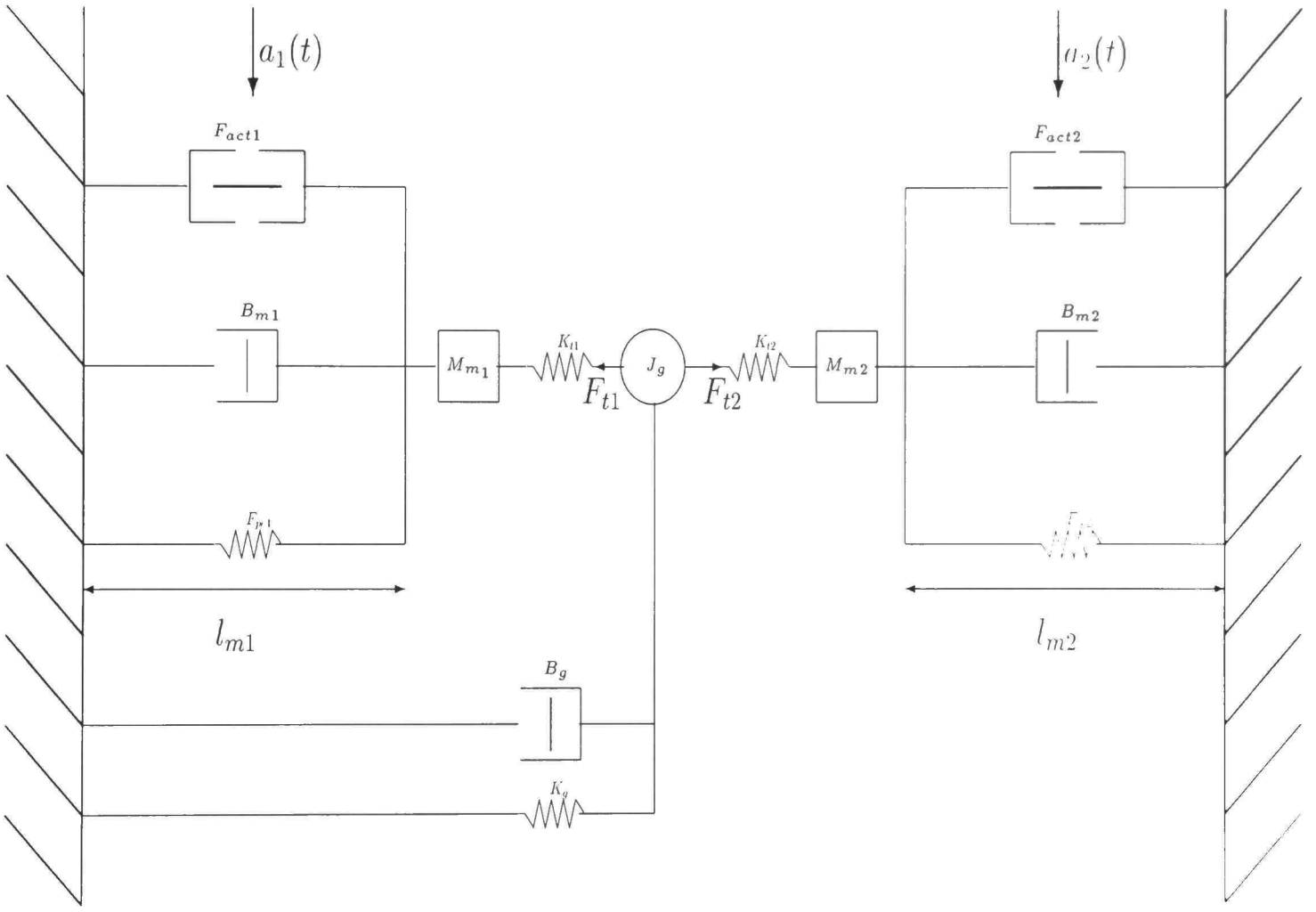

Figure 2.1: Occulomotor Plant

CHAPTER III
ANALYSIS OF THE SMOOTH TRACKING PROBLEM

In this chapter, the pursuit eye movement control, i.e.. control problem of visually tracking a slowly moving signal, is discussed. Attention is confined to the horizontal eye movement and the medial rectus and lateral rectus muscles are treated as actuators. It is evident that in most situations the dynamics of the signal to be tracked are unknown a priori. Therefore, the treatment begins with no assumptions on dynamics of the signal to be tracked. For control theoretic reasons. it becomes necessary to make some assumptions on the level of smoothness of the signal to be tracked. Here it is assumed that this signal is three times differentiable. Recall from the discussion in the introduction that according to Troost [23] the input signal to the occular motor control system during vestbulo-occular movement is the accleration of the head. Since the objective of the continuous control system during this phase is to keep the fovea fixed to a target (see the introduction) this input can be treated as the second derivative of the tracking signal. Thus, there is already physiological evidence to suggest that up to the second derivative of the tracking signal is involved in the occular motor control system. It is suggested here that further physiological research may needed to be carried out in order to verify whether or not the third derivative is also involved.

3.1 Tracking with a priori unknown dynamics

Here the problem of the eye tracking signal $\theta_r(t)$ is discussed where no assumptions are made regarding the details of the dynamics of $\theta_r(t)$. The only assumption made is that at time t the brain is aware of the value of θ_r and its first three derivatives. A physical example that would fit this description would be the motion of a fly. As had been stated in 4.2.1 it is assumed that the head is at rest at all times. The aim is to generate representative neural signals that will ensure that the eye angle $\theta(t)$

will track the reference signal $\theta_r(t)$ asymptotically. Let us rewrite the dynamics of the first two equations in (2.1) as

$$\begin{aligned} \dot{x}_1 &= x_2, \\ \dot{x}_2 &= -\frac{K_g}{J_g}x_1 - \frac{B_g}{J_g}x_2 + \frac{1}{J_g}(x_3 - x_4). \end{aligned} \tag{3.1}$$

where $x_1 = \theta$, $x_2 = \dot{\theta}$, x_3 and x_4 are the tendon forces of the medial and lateral rectus muscles. The aim here is to ensure that $x_1(t) - \theta_r(t) \to 0$ exponentially fast.

Let us temporarily treat $(x_3 - x_4)$ as a control input $v(t)$ to 3.1, so that it has the appearance of a second-order linear control system. It is also stable since its eigenvalues are at -51.0, -3109.0 corresponding to the assumed values of J_g, K_g and B_g. (These figures suggest a fairly high amount of damping and stiffness, and physiological reasons behind them are not clear from the literature) Therefore, the tracking problem can be solved if one were to take

$$v(t) = K_g\theta_r + B_g\dot{\theta}_r + J_g\ddot{\theta}_r, \tag{3.2}$$

for in this case, if the tracking error is defined as

$$(e_1, e_2) = (x_1 - \theta_r, x_2 - \dot{\theta}_r), \tag{3.3}$$

then the error dynamics satisfy

$$\dot{e}_1 = e_2 \tag{3.4}$$

$$\dot{e}_2 = -\frac{K_g}{J_g}e_1 - \frac{B_g}{J_g}e_2, \tag{3.5}$$

and this system has eigenvalues at $(-51.0, -3109.0)$.

Note that the third and fourth equations of (2.1) are.

$$\begin{aligned} \dot{x}_3 &= K_t(x_3)[-x_2 - (\frac{180}{\pi r})\dot{l}_{m_1}] \\ \dot{x}_4 &= K_t(x_4)[x_2 - \frac{180}{\pi r}\dot{l}_{m_2}. \end{aligned} \tag{3.6}$$

Since the function $K_t(.)$ is bounded from below, (3.6) can be solved for $\dot{l}_{m_1}$ and $\dot{l}_{m_2}$ for any desired expression for $\dot{x}_3$ and $\dot{x}_4$. The strategy here is as follows. As it

was argued earlier, $(x_3(t) - x_4(t))$ is needed to be controlled so that it will converge to the right hand side of (3.2) fast. This can be achieved by letting.

$$\dot{x_3} - \dot{x_4} = -\alpha(x_3 - x_4) + \dot{v}(t) + \alpha v(t). \tag{3.7}$$

where, α is a sufficiently large positive constant (α is chosen to be equal to 10 in the simulations to follow), and $v(t)$ is given in (3.2).

Define,

$$\begin{aligned} \gamma(t) &= \dot{v}(t) - \alpha v(t) && (3.8) \\ &= J_g \frac{d^3}{dt^3}\theta_r(t) + (B_g + \alpha J_g)\frac{d^2}{dt^2}\theta_r(t) + (K_g + \alpha B_g)\frac{d}{dt}\theta_r(t) + \alpha K_g \theta_r(t). && (3.9) \end{aligned}$$

Here the aim is to choose $\dot{l}_{m_1}$ and $\dot{l}_{m_2}$ such that the difference in the right hand sides of (3.6) is equal to the right hand side of 3.7. Solutions to this problem are clearly non-unique. This non-uniqueness has to be exploited to find physiologically realistic solutions. The relevant physiological constraints translate to the following:

1. muscle activations are in the range $[0, 1]$.
2. for small values of muscle activation the equation (3.6) cannot be inverted to solve for $\dot{l}_{m_i}$.

Additionally, physiological evidence has been reported to point out that the tendon forces never fall below a certain mimimum value.

In view of the above an arbitrary minimum value for the muscle tendon forces is fixed here (set at 10 gt in the simulations to follow). This bound is imposed indirectly via (3.6) by setting,

$$\begin{aligned} \dot{x_3} &= -\alpha x_3 + \gamma_1(t) \\ \dot{x_4} &= -\alpha x_4 + \gamma_2(t.) && (3.10) \end{aligned}$$

where γ_1 and γ_2 are always kept above α times the minimum tendon force. Due to the high bandwidth of (3.10) this ensures that $x_3(t)$ and $x_4(t)$ will seldom fall below the desired minimum value.

Let F_{min} = minimum muscle tendon force allowed. Now, the following limitations on γ_1 and γ_2 are imposed:

a) $\gamma_i(t) \geq (\alpha F_{min})$, $i = 1, 2$,

b) $\gamma_1(t) - \gamma_2(t) = \gamma(t)$, where $\gamma(t)$ is given in (3.9).

To meet these requirements choose $\gamma_i(t)$ as,

$$\gamma_1(t) = \begin{cases} \alpha F_{min} + \gamma(t), & \text{if } \gamma(t) \geq 0 \\ \alpha F_{min}, & \text{if} \gamma(t) < 0. \end{cases} \tag{3.11}$$

$$\gamma_2(t) = \begin{cases} \alpha F_{min}, & \text{if } \gamma(t) \geq 0 \\ \alpha F_{min} - \gamma(t), & \text{if} \gamma(t) < 0. \end{cases} \tag{3.12}$$

Finally, from (3.6) and (3.10), it follows that,

$$\dot{l}_{m_1} = \{\frac{1}{K_t(x_3)}[\alpha x_3 - \gamma_1(t)] - x_2\}\frac{\pi r}{180} \tag{3.13}$$

$$\dot{l}_{m_2} = \{\frac{1}{K_t(x_4)}[\alpha x_4 - \gamma_2(t)] + x_2\}\frac{\pi r}{180}. \tag{3.14}$$

where $\gamma_1(t)$ and $\gamma_2(t)$ are as in (3.11), $\gamma(t)$ is as in (3.9), and α is a reasonably large positive constant (choosen to be equal to 10 in the simulations).

Now, the muscle activations $a_1(t)$ and $a_2(t)$ are found by inverting (2.1). Of course these inversions will be valid only if the activations will fall in the range $[0, 1]$. Activations falling outside of the range will indicate either the attempted eye movement fall outside the physiologically feasible range, or that the feedback solution found here is inferior to the one employed physiologically. Simulations below illustrate that as long as the attempted eye movement is reasonable the proposed feedback law meet physiological constraints.

Assuming that the constraints are met, the muscle activations can be presented

as,

$$\begin{aligned} a_1(t) &= \frac{x_3(t) - F_{pe}(l_{m_1}(t))}{F_{max}F_l(l_{m_1}(t))[1 + (\frac{\dot{l}_{m_1}(t)}{V_{max}})^{1/3}]}. \\ a_2(t) &= \frac{x_4(t) - F_{pe}(l_{m_2}(t))}{F_{max}F_l(l_{m_2}(t))[1 + (\frac{\dot{l}_{m_2}(t)}{V_{max}})^{1/3}]}. \end{aligned} \tag{3.15}$$

where, $\dot{l}_{m_1}(t)$ and $l_{m_2}(t)$ are given in (3.14).

Observe that (3.15) describe muscle activation as a state feedback control law. It utilizes the first three derivatives of the reference signal. The neural inputs can be computed as,

$$n_i(t) = a_i(t) + \tau \dot{a}_i(t), \ i = 1, 2. \tag{3.16}$$

This completes the process of computing representative neural signals to the medial rectus and lateral rectus muscles during the pursuit of the reference signal $\theta_r(t)$.

3.2 Tracking with a priori known dynamics

Here, the case of following a signal which is generated as the output of a system with known dynamics, e.g., a rolling ball, is considered. The key assumption made is that the brain has an internal representation of the dynamics to be tracked. This is assumed to be of the form,

$$\dot{\omega} = S(\omega) \tag{3.1}$$

$$\theta_r = h(\omega), \tag{3.2}$$

where $\omega(t) \in \Re^n$, $\theta_r(t) \in \Re^n$, and S is a smooth function. By the same reasoning as in the previous section, θ_r and its first three derivatives are needed in order to compute

a feedback control law. In terms of the known dynamics these can be written as.

$$\theta_r = h(\omega) \tag{3.3}$$

$$\frac{d}{dt}\theta_r = L_s h(\omega) \tag{3.4}$$

$$\frac{d^2}{dt^2}\theta_r = L_s^2 h(\omega) \tag{3.5}$$

$$\frac{d^3}{dt^3}\theta_r = L_s^3 h(\omega). \tag{3.6}$$

These signals can be used in place of the explicitly computed derivatives here.

In order to illustrate this idea consider the simple example of tracking a ball rolling horizontally. Its dynamics have the form.

$$\dot{x_1} = x_2 \tag{3.7}$$

$$\dot{x_2} = -x_2. \tag{3.8}$$

where x_1 is the horizontal position of the ball, and x_2 is the velocity of the ball. For the sake of simplicity it is assumed that the mass of the ball and the applicable coefficcient of viscous friction are both equal to units. The eye keeps track of the location of the ball. Therefore, the output to be tracked is the angular position of the ball, which can be written as, $\theta_r(t) = \arctan(x_1/3)$, where 3 and is the distance from the eye to the line of motion of the ball.

Thus, the reference angle and its derivatives can be written as.

$$\begin{aligned}
\theta_r &= \arctan(x_1/3) \\
\frac{d}{dt}\theta_r &= \frac{3x_2}{3^2 + x_1^2} \\
\frac{d^2}{dt^2}\theta_r &= -\frac{3x_2(3^2 + x_1^2 + 2x_2x_2)}{(3^2 + x_1^2)^2}.
\end{aligned}$$

These expressions can be used in (3.9) in deriving the control laws given in (3.15).

3.3 Simulations

In this section, the performance of the feedback control law derived in (3.15) is illustrated via simulations. An 8^{th}-order model derived in [17] is used here, which is reproduced in (2.1) alongside with the values of the relevant parameters in Chapter II. Simulations were done in Matlab5 using ODE45 routines. These routines employ 2nd- and 4th-order Runge-Kutta method with adaptive step size control. The relevant Matlab program is included in the appendix.

In the simulations latency is interpreted as the time to "catch up" with the signal to be tracked reasonable well. Since no delays are explicitly modeled in the ocular motor plant (see Chapter II) simulations will not produce an explicit latency in response time. Most likely in reality there will be such a latency occuring due to cortical signal processing delays. It would be satisfactory for us in the simulations if the "time to catch up" is shorter that the maximum latency reported in Troost [23] of 125 msec during pursuit.

3.3.1 Tracking the movement of a sinusoidal signal

The problem of tracking the sinusoidal signal $\theta_r(t) = 20\ sin(2\pi t)$ for a 1.8 second time interval is considered. It is assumed that the eye initially start at 10^0 angular position. Simulation results are shown in Figure 3.1

First, the simulation demonstrate that the designed controller acomplishes pursuit eye movement very well. Figure 3.1.a shows that the tracking error is practically equal to zero after about 40 msec. Tendon forces (Figure 3.1.b), muscle lengths (Figure 3.1.c) and activation signals (Figure 3.1.d) are well within the designed limits.

It is seen in Figure 3.1.a that in about 40 msec the eye catches up with the signal to be tracked. This is well within the maximum latency of 125 msec reported by Troost in [23]. The peak eye velocity is around 200^0/sec which is more than the reported maximum value of 50^0/sec. Note that the occular motor system is capable of

generating such speeds during saccadic eye movement. Therefore, this peak velocity doesn't inherently violate physical limits of the system. We would like to offer the following interpretation in this regard. In the control design no attempt was made to exactly match the actual neural signals since they are not known to us. The control design presented only describe the capabilities of the muscular-occular-motor system. It is very likely that the cortex has its own bandwidth limitations, and the reported velocity limits are due to those. If one would like to obtain a better fit he could play with the parameter α in the controller, and with placing eigenvalues in 3.5 closer to the imaginary axis.

3.3.2 Tracking the movement of a ramp signal

The problem of tracking the ramp signal $\theta_r(t) = 15t$ for a two second time interval is considered. It is assumed that the eye initially start at 10^0 angular position. Simulation results are shown in Figure 3.2

Simulation results show that the controller works very well while respecting tendon force, muscle length and activation level limits. The latency is about 40 msec and the peak eye velocity is about 250^0/msec. Again, these results show that the performance of the controller is slightly superior to the physiologically observed performance reported in Troost [23]. The explanation offered in the same as in the previous example.

3.3.3 Tracking the movement of a ramp signal

It turns out that the parameter α in the designed control law play an important role in keeping the activation signals within reasonable bounds. Here the problem considered in section 3.3.2, i.e., tracking a ramp signal of amplitude 30^0 in two seconds, is revisited. The parameter α is set to 2 (instead of 10 as in other examples). Angular variables and the activation signals are plotted in Figure 3.3.

Clearly the results shown are unacceptable due to excessive activation levels required. This accomplishes our objective which was to show that the parameter a used in the control design cannot be too low.

3.3.4 Tracking the movement of a quadratic signal

The problem of tracking the signal $\theta_r(t) = 5t^2$ for a two-second time interval is considered. It is assumed that the eye initially start at 10^0 angular position. Simulation results are shown in Figure 3.4.

Simulation results show that the designed controller works well, but its performance is superior to physiologically observed results. Explanation given in section 3.3.1 is applicable here as well.

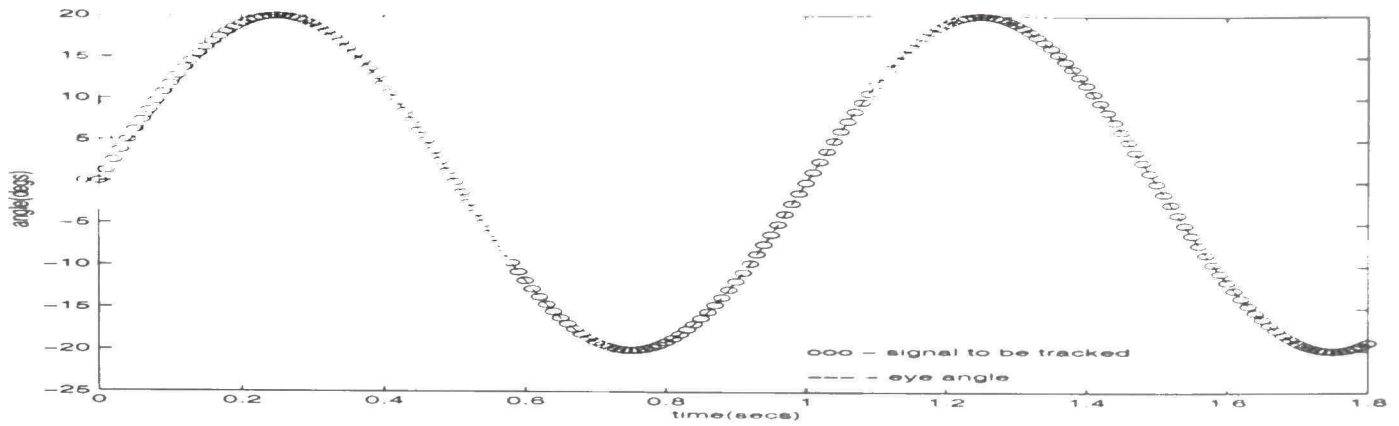

(a) Angles

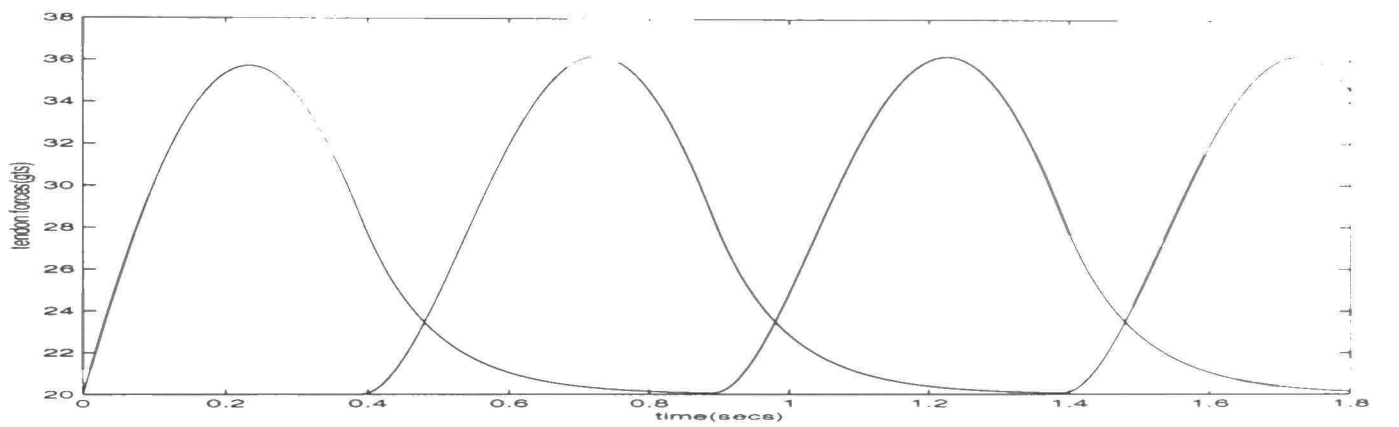

(b) Tendon Forces

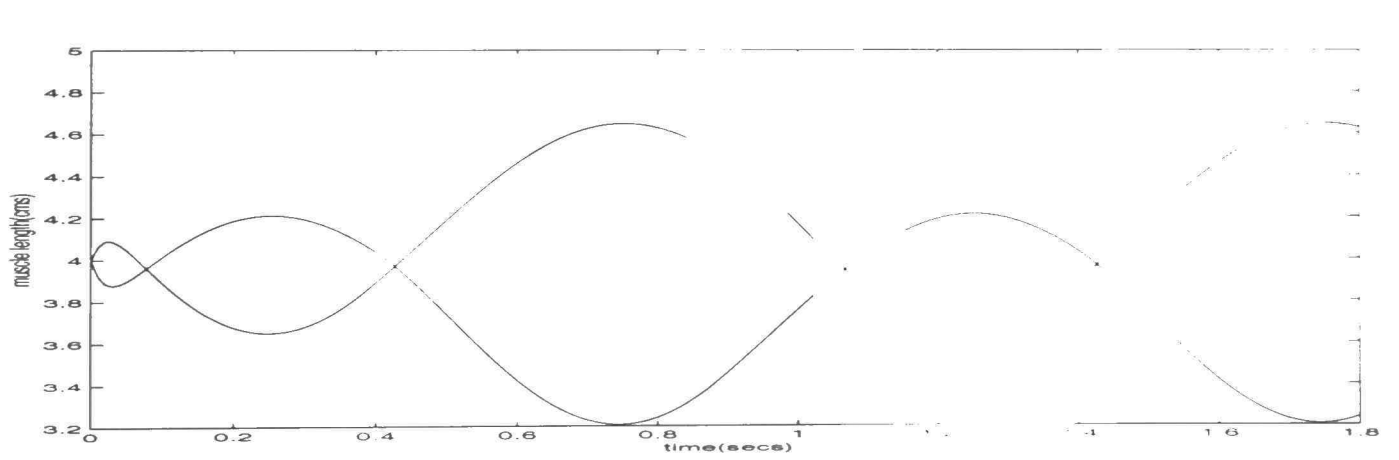

(c) Muscle Lengths

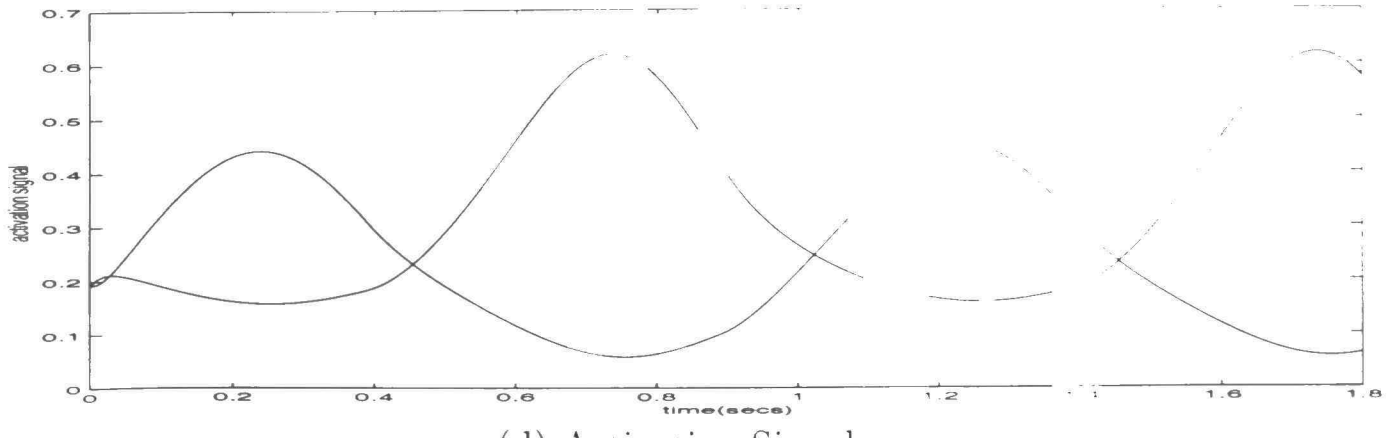

(d) Activation Signals

Figure 3.1: Tracking a sinusoidal signal $\theta_r(t) = 20.0\ sin(2\pi t)$

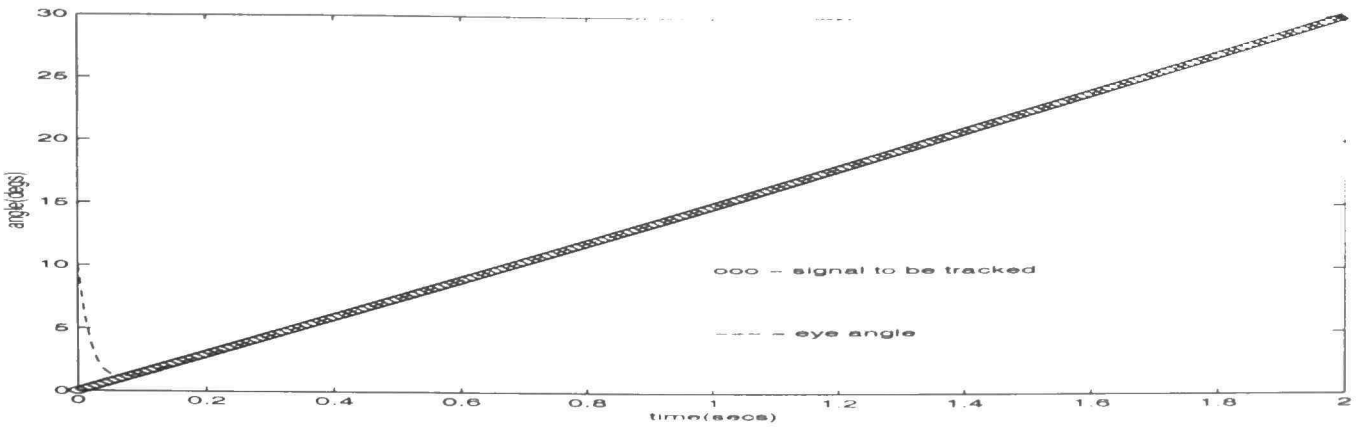

(a) Angles

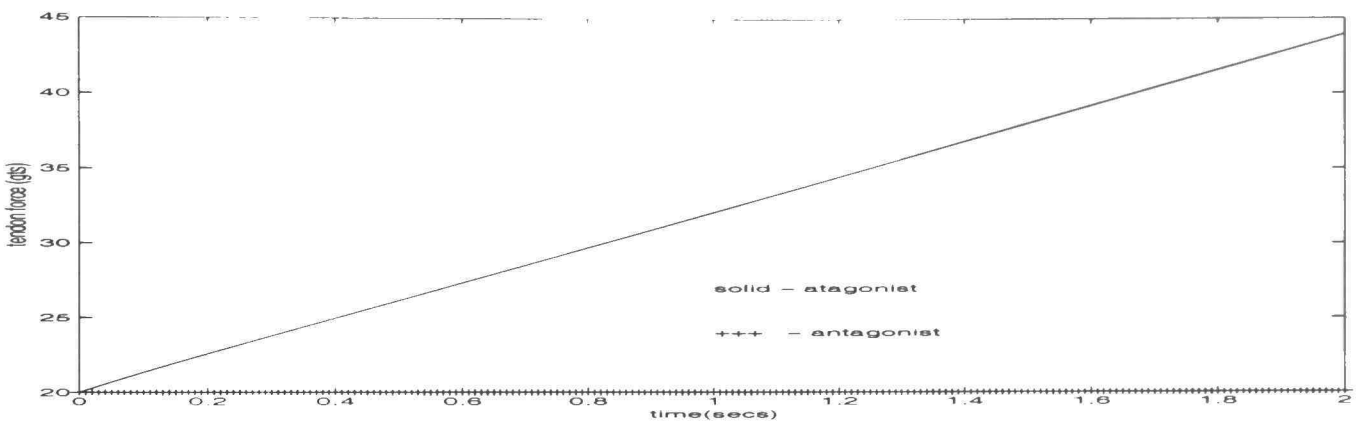

(b) Tendon Forces

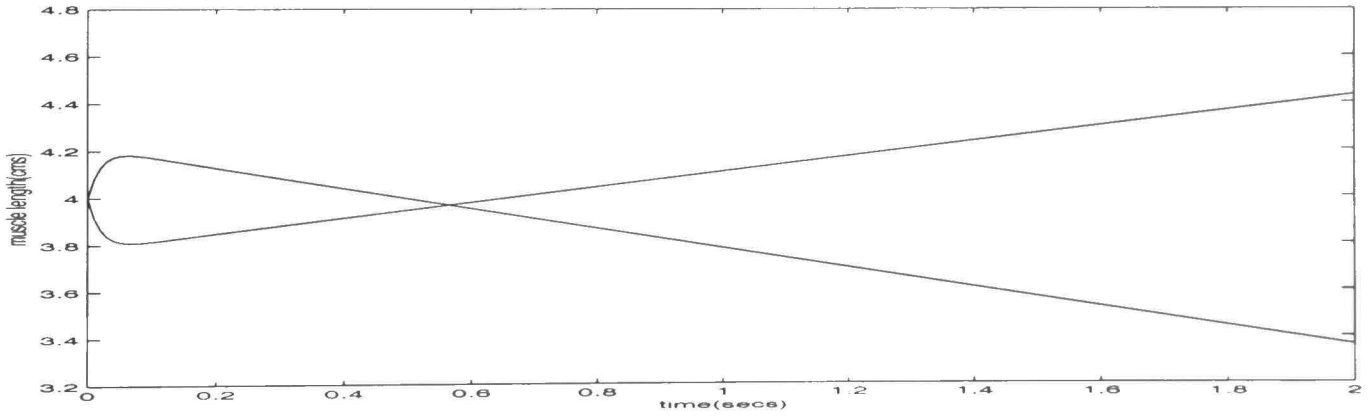

(c) Muscle Lengths

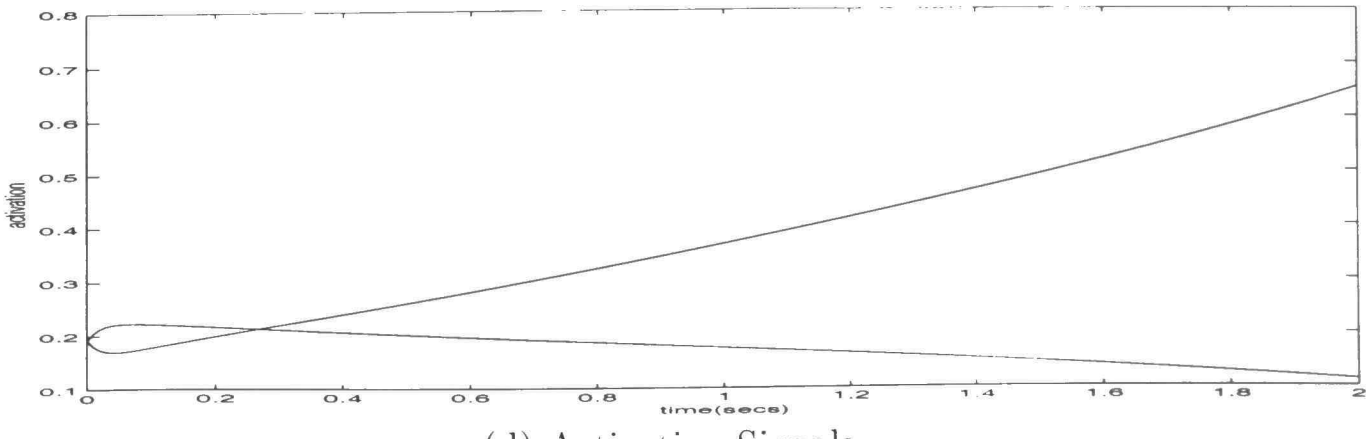

(d) Activation Signals

Figure 3.2: Tracking a ramp signal $\theta_r(t) = 15t$

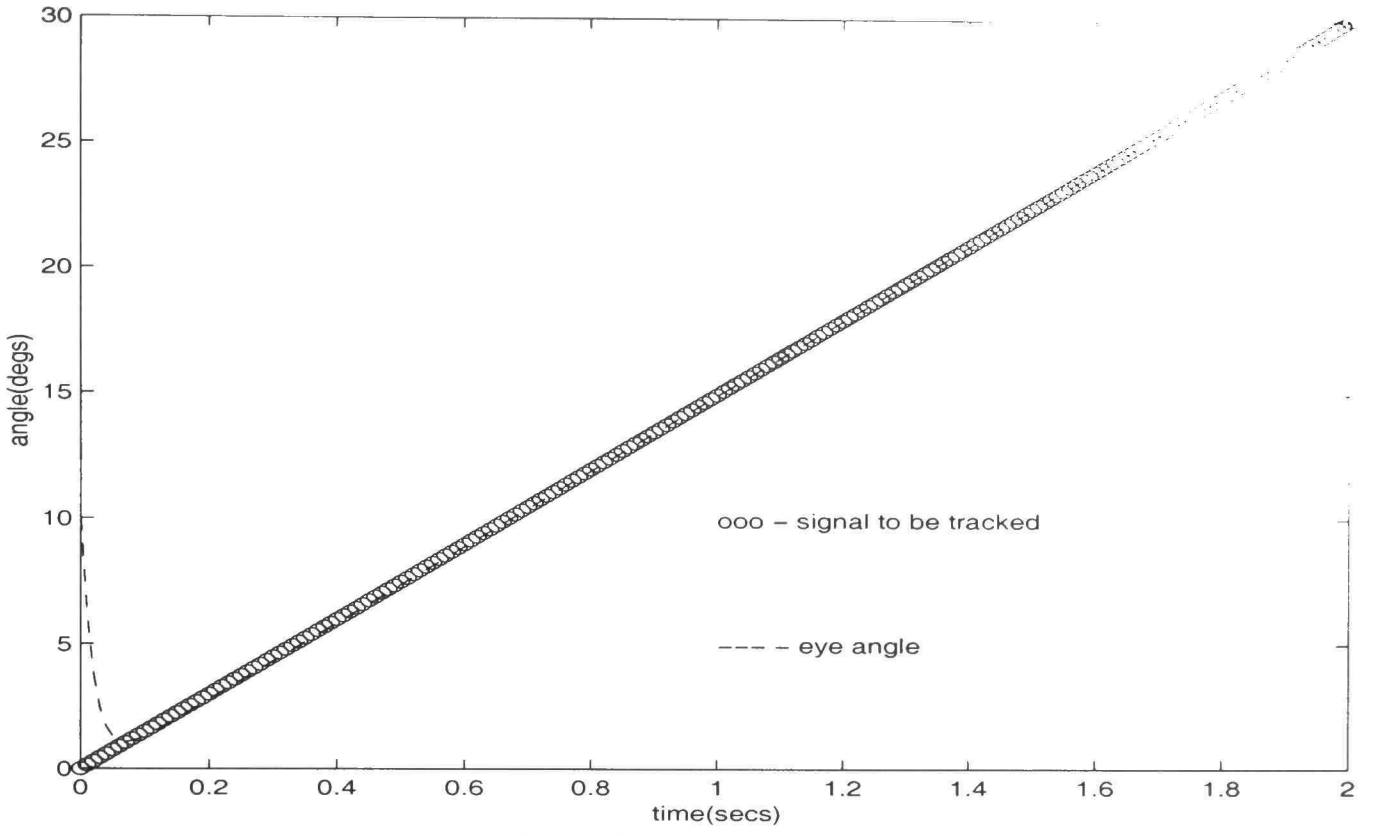

(a) Angles

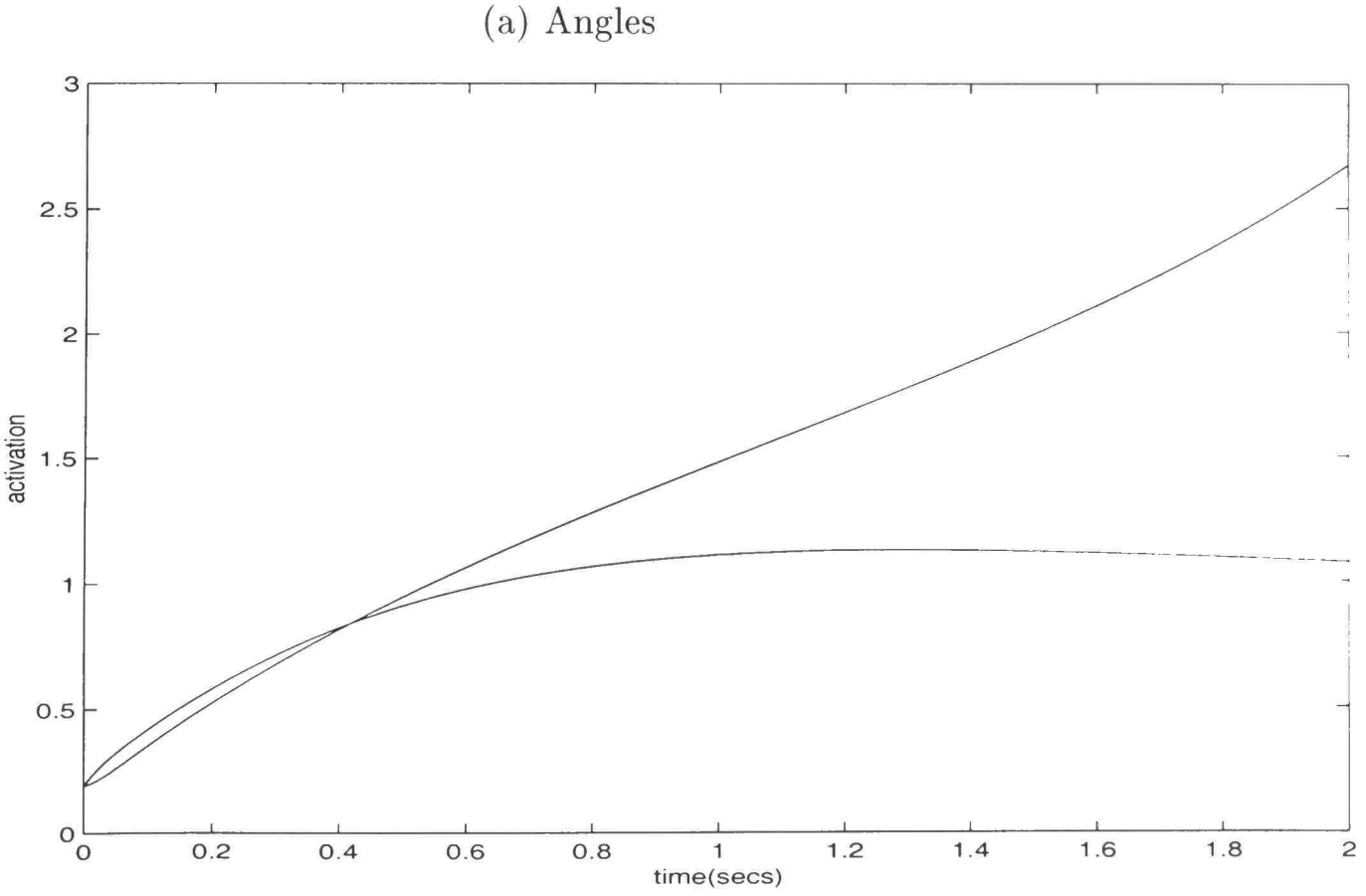

(d) Activation Signals

Figure 3.3: Tracking a ramp signal $\theta_r(t) = 15t$ with $\alpha = 2$

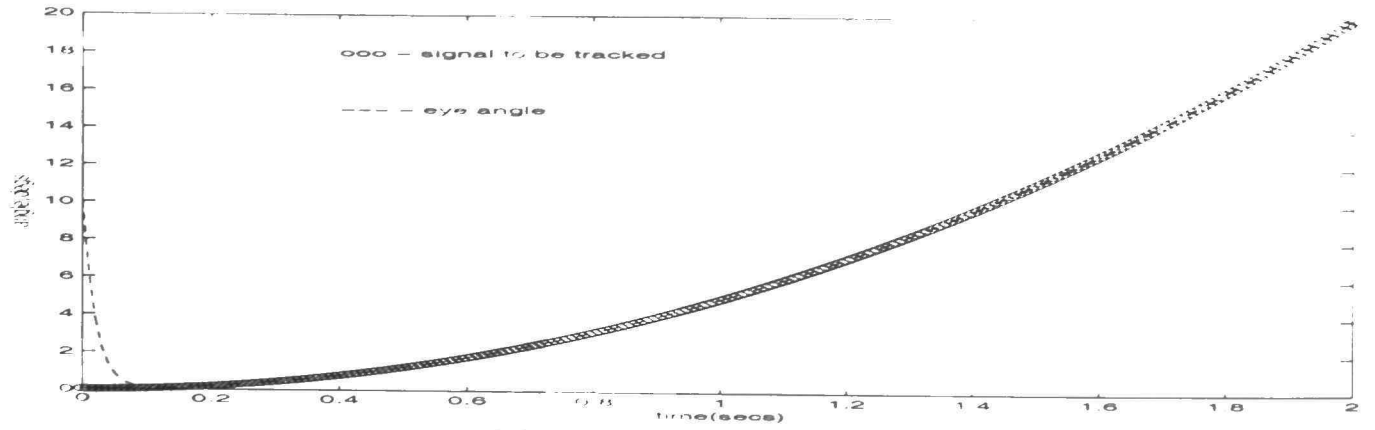

(a) Angles

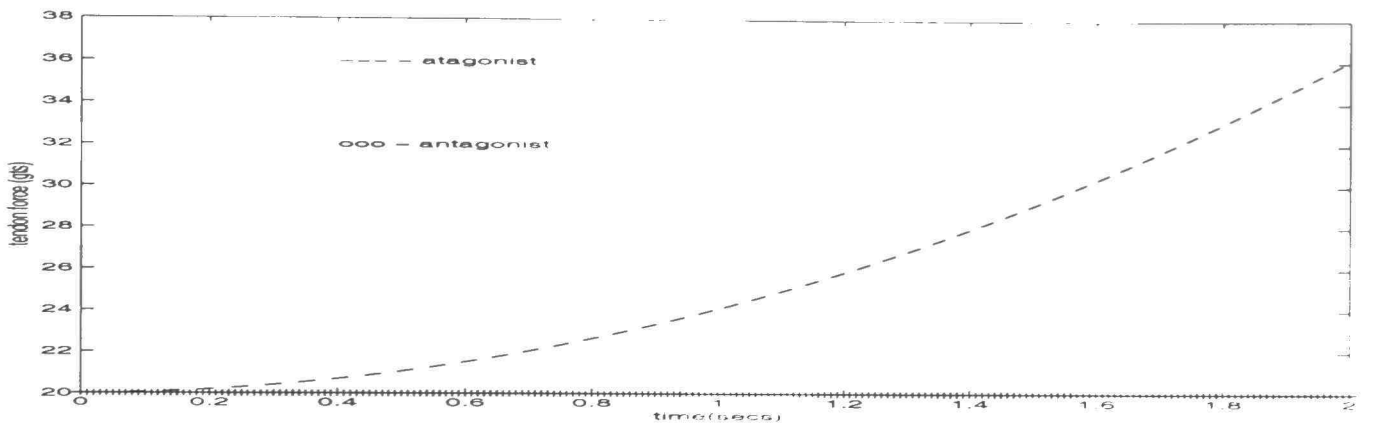

(b) Tendon Forces

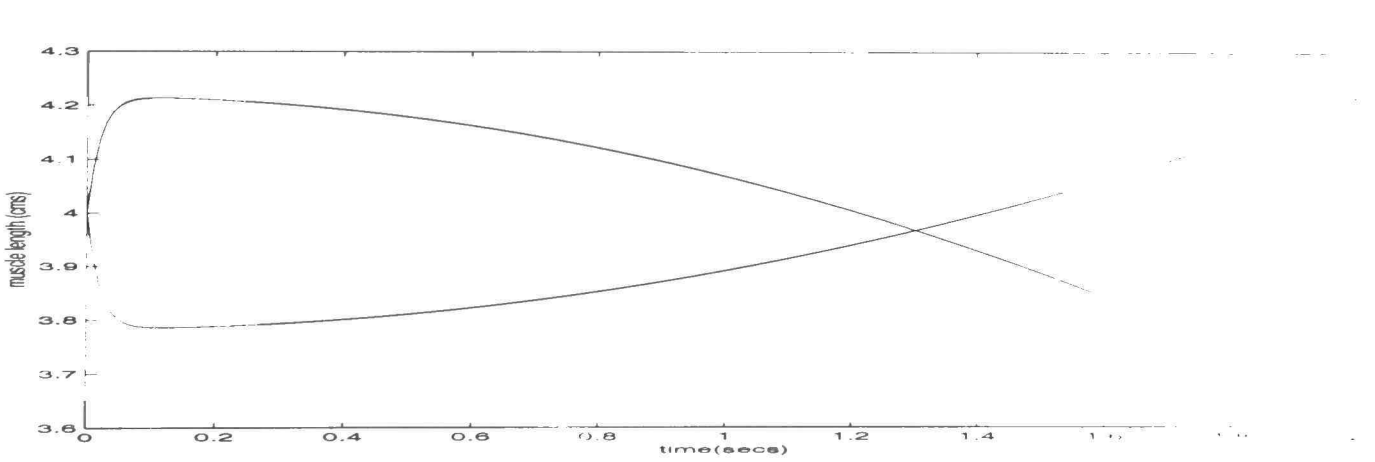

(c) Muscle Lengths

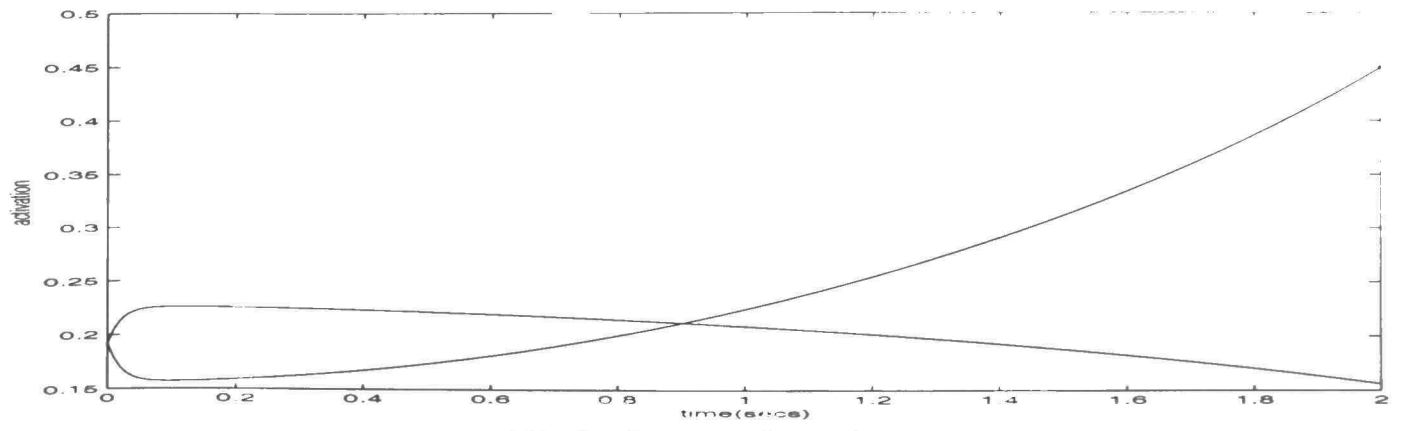

(d) Activation Signals

Figure 3.4: Tracking a quadratic signal $\theta_r(t) = 5t^2$

CHAPTER IV
CONCLUDING REMARKS

The objective of this thesis is to study the pursuit eye movement from the perspective of control theory. To be specific, a representative control law was designed to accomplish pursuit eye movement utilizing an oculomotor plant model developed in [17] and via simulations it was demonstrated that the control law can accomplish this task. Plant model utilized take into consideration anatomically realistic models of muscular actuators, but ignore cortial detals.

Hitherto pursuit eye movement has not been studied with the same vigor as the saccadic eye movement, and no reasonable data seem to be available to even compare the performance of the designed controller with physiological observations. Yet, sketchy details on latency and peak velocity during pursuit reported by Troost etc. (see e.g [23]) seem to indicate that the designed controller performs slightly better than the physiological controller, and the most likely reason is that the cortical circuitry impose additional restrictions on the speed of tracking.

The key ideas behind the design of the pursuit controller here can be extended to study vergence and vestibulo-occular control eye movements as well. It is our hope to carry this out in the future. It is also hoped that the validity of the general nature and the performance will be checked via physiological experiments in the future.

BIBLIOGRAPHY

[1] Robinson D. A. The mechanics of human saccadic eye movement. *Jounal of Physiology*. 174:245–264, 1964.

[2] Robinson D. A. *Models of mechanics of eye movements*. CRC Press. 1981.

[3] Robinson D. A., D. M. O'Meara, A. B. Scott, and Collins C. C. Mechanical components of human eye movements. *Journal of Applied Physiology*. 26(5):548–553, 1969.

[4] Bach-y-Rita(ed). *Orbital Mechanics*. Pergammon Press. Oxford. 1975.

[5] A. T. Bahill and B. T. Troost. Types of saccadic eye movements. *Neurology*. 29:1150–1152, 1979.

[6] M. R. Clark and L. Stark. Control of human eye movements: I.modelling of extraocular muscles; ii. a model for the extraocular plant mechanism: iii. dynamic characteristics of the eye tracking mechanism. *Mathematical Biosciences*. 20:91–265, 1974.

[7] C. Collins. The Control of Human Eye Movements. pp. 145–180. In Bach-y-Rita [4], 1975.

[8] G. Cook and L. Stark. Derivation of a model for the human eye-positioning mechanism. *Bull. Math. Biophys.*, 29:153–174, 1967.

[9] P. Cooke. *A Dynamic 3D Model of the Human Eye Movement*. PhD Dissertation. Texas Tech University, 1998.

[10] R. Descartes. *Treatise of Man (T. S. Hall (trans)*. Harvard University Press. Cambridge. MA, 1972.

[11] M. Egerstedt. A model of the combined planar motion of the human eye. Master's thesis, Royal Institute of Technology, Stockholm, Sweden. 1996.

[12] B. Fisher. Express saccades laboratory publications (web page: University of Freiburgh). *http://www.brain.uni-freiburg.de/fisher/pubs*.

[13] J. He. *A feedback control analysis of the neuro-musculo-skeletal system of a cat hindlimb*. PhD Dissertation. University of Maryland, 1988.

[14] A. V. Hill. The heat of shortening and dynamic constants of muscle. *Proc. Roy. Soc. Lond.,*. (B126):136–195, 1938.

[15] R. J. Leigh and D. S. Zee. *The Neurology of Eye Movements*. Contemporary neurology series. 55. Oxford University Press, New York. 3rd ed edition. 1999.

[16] C. F. Martin and L. Schovenec. The control and mechanics of human movement systems. *Dynamical Systems Control, Coding, Computer Vision. New Trends, Interfaces, and Interplay. Progress in Systems and Contro*. 25:173–203. 1999.

[17] A. McSpadden. A 2d dynamic model of human eye movement. Master's thesis, Texas Tech University, Lubbock, Texas. 1998.

[18] A. McSpadden, C. F. Martin, and L. Schovenec. A model of the saccadic eye movement system: Effects of nonlinear muscle mass. *Mathematics of Bioscience*. submitted.

[19] K. Rayner. *Eye Movements and Visual Cognition*. Springer-Verlag, New York. 1992.

[20] R. Robleto. An analysis of the musculotendon dynamics of hill-based models. Master's thesis, Texas Tech University, Lubbock, Texas. 1997.

[21] R. H. Specter and B. T. Troost. The oculomotor system. *Ann. Neurol.*, 5:517–525. 1981.

[22] S. Squatrito and M. G. Maioli. Encoding of smooth pursuit direction and eye position by neurons of area MSTD of macaque monkey. *The Journal of Neuroscience*, 17:3847–3860. 1997.

[23] B. T. Troost. Introduction to human eye movement control (web page) . *http://www.toddtroost.com/lectures/eyemove/elec.html*.

[24] B. T. Troost. An overview of oculomotor neurophysiology. *Ann. Otol. Rhinol. Laryngol.*, 4 part 3 suppl 86:29–36, 1981.

[25] B. T. Troost, R. B. Neber, and R. B. Daroff. Hemispheric control of eye movements. i: Quantitative analysis of refixation of saccades in a hemispherectomy patient. *Arch. Neurol.*, 27:449–452. 1972.

[26] B. T. Troost, R. B. Neber, and R. B. Daroff. Hemispheric control of eye movements. ii: Quantitative analysis of smooth pursuit in a hemispherectomy patient. *Arch. Neurol.*, 27:442–448. 1972.

[27] F. E. Zajac and Levine W. S. Neuromuscular and musculoskeletal control models for the human leg. *Proc. 1983 ACC.* pp. 229 234. June 1983.

```
%Function theta_ref_vec allows the user to specify the
%reference signal to be tracked and its first three derivatives.
%In the example below a sinusoidal signal is specified.
%User should edit theta(1),···,theta(4) below in order
%to describe a different reference signal.
function theta = theta_ref_vec(t)
        omega = 1.0;
       p = 2.0*3.1415926535;
        amplitude = 20.0;
        theta(1) = amplitude*sin(p*t); %reference signal (eye angle theta_ref(t)
        theta(2)=  p*amplitude*cos(p*t);  % (derivative of reference signal (dot_
        theta(3) = -p*p*amplitude*sin(p*t); % dot_dot_theta_ref(t)
        theta(4) = -p*p*p*cos(p*t);  % dot_dot_dot_theta_ref(t)
```

```
%This main routine specifies parameter values of the oculomotor plant
%model given in Table 2.1,  specify initil conditions,
% specify the time interval, call ode45 to do the simulation
%(note:internal routines call the control design algorithm here)
%and process and store  data to a form suitable for plotting.
global Bpm
          Bpm = 0.06;
global Bg
          Bg = 0.0158;
```

```
global Kg
          Kg = 0.79;
global Jg
         Jg = 0.000005;
global M
        M= 0.748;
global r
        r = 1.24;
global lms
        lms = 3.7;
global lmc
        lmc = 4.8;
global kme
        kme= 0.0387;
global kml
        kml = 0.126;
global kpm
        kpm = 0.9;
global Fmc
        Fmc = 20.0;
global Fmax
        Fmax = 100.0;
global Ftc
        Ftc = 30.0;
global lopt
        lopt = 4.65;
global w
        w = 0.5;
global kte
```

```
        kte = 0.0333;
global ktl
        ktl = 1.5;
global ks
        ks = 2.5;
global tau
        tau = 0.002;
global ltc
        ltc =0.532;
global lts
        lts =0.2;
global Vmax
        Vmax = 5689.0;
global alpha
        alpha = 10.0;
%initial state
x0 =[10.0, 0,  20, 20, 4.0,4.0];
%x0 = [0,0,4,0,4,0,2.2,2.2,0.0,0.0];
%x0=[5.0,0,4,0,4,0,2.31141,2.31141,0,0];
%initial time for the simulation
t0 = 0.0;
%final time for the simulation
tf = 1.8;
%call ode45 routine to cary out the simulation.
[t,x] = ode45('model_red_track',[t0:0.01:tf],x0);
%calculate activation forces from what has been computed already.
pp = post_process_act_calc(t,x);
x(:,7) = pp(:,1);
x(:,8) = pp(:,2);
```

```
x(:,9) = pp(:,3);
x(:,10) = pp(:,4);
fid = fopen('output','w');
%Store computed data in the file output.
fprintf(fid,'%8.3f %8.3f %8.3f %8.3f %8.3f %8.3f %8.3f %8.3f %8.3f %8.3f
n',x);
fclose(fid);



%Function Kt  correspont to the equation (2.3) in the
%occulomotor plant model described in Chapter 2.
function zz = Kt(x7)
global kte;
global ktl;
global ks;
global ltc;
global lts;
global r;
Ftc = (ktl/kte) * ( exp( (180.0/(pi*r))*kte*(ltc-lts) ) -1.0 );
switch x7
        case x7 <0
                zz = 0.0;
        case x7 > Ftc
                zz = ks;
        otherwise
                zz = kte*x7 + ktl;
end
```

```
% Function Fpe corresponds to the equation (2.6) in the
%occulomotor plant model described in Chapter 2.
function yy = Fpe(z)
        global lmc;
        global lms;
        global kpm;
        global kml;
        global kme;
        global Fmc;
        global r;
switch z
                case (z < lms)
                        yy = 0.0;
                case (z > lmc)
                        yy = kpm*180.0/(pi * r) * (z - lc) + Fmc;
                otherwise
                        yy = (kml/kme) * (exp ( kme * (180.0 / (pi * r))* (z - lm
        end


% Function Fl corresponds to equation (2.7) in the
%occulomotor plant model described in Chapter 2.
function z = Fl(lm)
        global lopt;
        global w;
        lmbar = lm/lopt;
        zz = 1.0 - (lmbar-1)*(lmbar-1)/(w*w);
        z = max(0,zz);
```

```
%Function F_t_diff computes v(t)  in equation (3.2)  and its
%derivative. These are used in equation (3.9) in the
%control design.

function ftdiff = F_t_diff(t)
        global Jg;
        global Bg;
        global Kg;
        xx=theta_ref_vec(t);
        ftdiff(1) = Jg*xx(3) + Bg*xx(2)+Kg*xx(1);
        ftdiff(2) = Jg*xx(4) + Bg*xx(3)+Kg*xx(2);
```

```
%Function lm_vec computes l_m1 and l_m2
%used in the control design in equations (3.14).
function lm_vec = lm_dot_1_2(t,x2,x3,x4,r,Jg,Bg,Kg,alpha,kte,ktl,ks,ltc,lts)
        global r;
        global Jg;
        global Bg;
        global Kg;
        global alpha;
        global kte;
        global ktl;
        global ks;
        global ltc;
        global lt;
```

```
minimum = 200;
eps1 = -0.0001;

vv = F_t_diff(t);
gamma_diff = + alpha*vv(1) + vv(2);
if ( gamma_diff > eps1)
        gamma_1 =  minimum+gamma_diff;
        gamma_2 = minimum;
else
        gamma_1 = minimum;
        gamma_2 = minimum-gamma_diff;
end

kt_1 = Kt(x3);
kt_2= Kt(x4);
        c1=(pi*r/180.0);

        lm_vec(1) = c1* (  (-gamma_1 + alpha*x3)/kt_1  - x2);
        lm_vec(2) = c1* ( (-gamma_2 + alpha*x4)/kt_2  +x2);


%Function model computes the first six
%elements in the right hand side of the oculomotor plant
% model given in equation (2.1).
function xd = model(t,x)
global Bpm;
global Bg;
global Kg;
global Jg;
```

```
global M;
global r;
global lms;
global lmc;
global kme;
global kml;
global kpm;
global Fmc;
global Fmax;
global lopt;
global w;
global kte;
global ktl;
global ks;
global tau;
global ltc;
global lts;
global Vmax;
global alpha;
lmm_dot = lm_dot_1_2(t,x(2),x(3),x(4));
xd(1) = x(2);
xd(2) = (x(3) - x(4) - Bg*x(2) -Kg * x(1))/Jg;
xd(3) = Kt(x(3)) *(-x(2) - (180.0/(pi*r))*lmm_dot(1) );
xd(4) =Kt(x(4)) *(x(2) - (180.0/(pi*r))*lmm_dot(2) );
xd(5) = lmm_dot(1);
xd(6) = lmm_dot(2);
xd = xd';
```

```
%Function post_process_act_calc computes
%activation forces from what has been computed already.
function pp = post_process_act_calc(t,x)
global lmc;
global lms;
global kpm;
global kml;
global kme;
global Fmc;
global Fmax;
global r;
global Jg;
global Bg;
global Kg;
global alpha;
global kte;
global ktl;
global ks;
global ltc;
global lts;
global Vmax;
global w;
global lopt;



  maximum = 10000;
```

```
eps1 = 0.0001;
n = size(x,1);
for i=1:n
      p1 =x(i,3) - Fpe(x(i,5));
      p2 =x(i,4) - Fpe(x(i,6));
      theta_r = theta_ref_vec(t(i));
      lm_vec = lm_dot_1_2(t(i),x(i,2),x(i,3),x(i,4));
      fl1= Fl(x(i,5));
      fl2 = Fl(x(i,6));
      den1= Fmax*fl1*(1+lm_vec(1)/Vmax)^(1/3);
      den2=Fmax*fl2*(1+lm_vec(2)/Vmax)^(1/3);
      pp(i,1) =maximum;
      pp(i,2) = maximum;
      pp(i,3) = x(i,1) - theta_r(1);
      pp(i,4) = theta_r(1);
      if(abs(den1)>eps1)
            pp(i,1) = p1/den1;
      end
      if(abs(den2) > eps1)
            pp(i,2) = p2/den2;
      end

 end


% Plot muscle activation forces.

plot(t,x(:,7),t,x(:,8))
```

```
% Plot eye angles.
plot(t,x(:,1), t,x(:,9), t,x(:,10))

% Plot tendon forces
plot(t,x(:,1), t,x(:,9), t,x(:,10))
```

PERMISSION TO COPY

In presenting this thesis in partial fulfillment of the requirements for a master's degree at Texas Tech University or Texas Tech University Health Sciences Center, I agree that the Library and my major department shall make it freely available for research purposes. Permission to copy this thesis for scholarly purposes may be granted by the Director of the Library or my major professor. It is understood that any copying or publication of this thesis for financial gain shall not be allowed without my further written permission and that any user may be liable for copyright infringement.

Agree (Permission is granted.)

[signature]	7/20/99
Student's Signature	Date

Disagree (Permission is not granted.)

Student's Signature	Date